On bifurcations in reaction-diffusion systems in chaotic flows

Shakti N. Menon and Georg A. Gottwald *
School of Mathematics & Statistics, University of Sydney,
NSW 2006, Australia.

Abstract

We study the behaviour of reacting tracers in a chaotic flow. In particular, we look at an autocatalytic reaction and at a bistable system which are subjected to stirring by a chaotic flow. The impact of the chaotic advection is described by a one-dimensional phenomenological model. We use a non-perturbative technique to describe the behaviour near a saddle node bifurcation. We also find an approximation of the solution far away from the bifurcation point. The results are confirmed by numerical simulations and show good agreement.

PACS numbers: 82.40.Ck, 05.45.-a, 82.40.Bj, 47.52.+j

*corresponding author: gottwald@maths.usyd.edu.au

1 Introduction

In recent years, interest has risen in the dynamics of reacting tracers in a complex flow environment. Apart from the purely theoretical challenge, this is due to the environmental and industrial applications. Examples are ubiquitous in nature and industry, and include mixing of reactants within continuously fed or batch reactors [1, 2], the development of plankton blooms and occurrence of plankton patchiness [3, 4, 5, 6], and increased depletion of ozone caused by chlorine filaments [7].

In typical chaotic flows, fluid parcels are deformed. Chaotic advection gives rise to regions of stretching and folding, causing fluid parcels to form filamental structures. Tracers are advected with these filaments, which leads to an increased surface area of the tracers. In the case of reacting tracers, this has strong implications on the reaction kinetics and gives rise to new phenomena which are not observed in a non-stirred flow. For example, differential fluid flow can generate a non-Turing mechanism for pattern formation [8], chaotic flow can determine synchronization in oscillatory media [9, 10] or cause clustering [11]. Chaotic stirring also implies a dependence of mixing results on the initial condition [12].

In principle, these phenomena can be studied directly in a $2D$ or $3D$ reaction-advection-diffusion system with huge computational effort. An analytical treatment of the full system is prohibited by the complicated nature of the underlying equations, which involve multiple-scale processes. Simplified models are needed to capture essential features of the influence of the stirring on the reaction kinetics. Such a model was first introduced in [4, 5]. They replaced the two-dimensional problem of reacting tracers by a one-dimensional one of the form

$$\frac{\partial}{\partial t}c_i - \lambda x \frac{\partial}{\partial x}c_i = D_i \frac{\partial^2}{\partial x^2}c_i + \mathcal{F}_i(c_i, k_i) \ , \tag{1}$$

for n reacting tracers, c_i, with diffusion coefficients D_i, reaction rates k_i and stirring rate λ. A single reacting tracer with $\mathcal{F}(c) = c$ and $\mathcal{F}(c) = c(1-c)$ was studied in [4] and [5], but the idea has been taken up by several authors and was applied to more interacting tracers in bistable and excitable media in several physical, chemical and biological contexts [13, 14, 15, 16, 17, 18]. The phenomenological model (1) can be justified by the following consideration: The chaotic advection causes filaments to be stretched in one direction and compressed in another. In the stretched direction, the concentration is homogenized and gradients along the filaments can be neglected. This motivates a one-dimensional reduction for the concentration in the direction transverse to the filament, subject to the effect of stirring and compression. The parameter λ can be thought of as the Lagrangian mean strain in the contracting direction, and is given by the absolute value of the negative Lyapunov exponent. For a different approach to this problem see [19].

In [13, 14, 15, 16, 17, 18], it was numerically shown that the behaviour of the one-dimensional filament model (1) qualitatively describes the behaviour of the respective full $2D$ reaction-advection-diffusion system. In particular, a saddle node bifurcation was observed. The saddle node can be phenomenologically understood as the competition of stirring and reaction. If the stirring is too strong, i.e. it occurs on a faster time scale

than the reaction, the filaments become thin and (in the case of a closed flow) soon cover the whole fluid container, or (in the case of an open flow) leave the fluid container. Consequently, perturbations are either carried out of the container, or filaments are too thin to cause spread of reaction. In some cases, an asymptotic theory could be developed for slow stirring rates, λ, far away from the saddle node [14]. However, the bifurcation point and the pulse behaviour close to the saddle node has not been previously described. We use a non-perturbative, non-asymptotic technique developed for excitable media in [20] to describe the behaviour near the saddle node. We consider a bistable and an autocatalytic system, and determine the critical bifurcation parameter and the pulse shape close to the bifurcation point, as a function of the equation parameters. Moreover we apply the same technique to describe the form of the solution far away from the bifurcation point going beyond the asymptotic analysis of [14].

In the next Section, we present the two models which under consideration. In Section 3 we review the perturbation technique developed in [20], and in Section 4 we show results of our perturbation technique for the models presented in Section 2 close to the saddle node bifurcation, and compare with numerical results. In Section 5 we find an approximate solution for the front solutions far away from the bifurcation point.

2 The models

We use two different one-component models to illustrate our method. We study the same models used in [14]. Therein also, the behaviour of the full $2D$ reaction-advection-diffusion systems for closed and open chaotic flows was investigated. We follow their notation and rescale Eq. (1) by introducing non-dimensional variables $t' = \lambda t$ and $x' = \sqrt{\lambda/D}x$ to obtain (omitting the primes)

$$\frac{\partial}{\partial t}c - x\frac{\partial}{\partial x}c = \frac{\partial^2}{\partial x^2}c + Da\ \mathcal{F}(c)\ , \tag{2}$$

where the Damköhler number $Da = k/\lambda$ measures the ratio of the time scales of fluid motion and reaction, respectively. Small Damköhler numbers correspond to fast stirring/slow reaction. For large Damköhler numbers, the system behaves asymptotically like an unstirred system.

For the reaction term $\mathcal{F}(c)$, we use the Fisher-Kolomogorov-Petrovsky-Piscounoff (F-KPP) type [21, 22]

$$\frac{\partial}{\partial t}c - x\frac{\partial}{\partial x}c = \frac{\partial^2}{\partial x^2}c + Da\ c(1-c)\ . \tag{3}$$

This equation has two equilibrium points: an unstable fixpoint, $c = 0$, and a stable one, $c = 1$. It describes the propagation of an unstable phase into a stable phase. The reaction term arises naturally for autocatalytic reactions $A + B \to 2B$, and was first introduced in the context of population dynamics in [21] and in the context of combustion in [22].

Eq. (3) has recently been used as a caricature to model plankton blooms [4].

As a second model we introduce a generic bistable model

$$\frac{\partial}{\partial t}c - x\frac{\partial}{\partial x}c = \frac{\partial^2}{\partial x^2}c + Da\; c(\alpha - c)(c-1)\;, \tag{4}$$

where $0 < \alpha < 1$. This system has two stable fixed points, $c = 0$ and $c = 1$, which are separated by an unstable fixed point at $c = \alpha$. it is well known that in the unstirred case an initial perturbation which is larger than α over a finite range will spread over the whole domain if $0 < \alpha < 0.5$. If $0.5 < \alpha < 1$, an initial perturbation will decay to the stable state $c = 0$.

For the non-stirred case, both systems are well known and well described in textbooks such as [23, 24, 25, 26]. The stirred cases were investigated numerically in [14, 5]. In the stirred case stationary fronts exist for large enough values of the Damköhler number for both models. The existence of stationary fronts in systems (3) and (4) is due to a balance of the x-dependent stirring and the counterpropagating fronts. An initial sufficiently large perturbation seeded at $x = 0$ spreads as a front driven by its reaction kinetics and diffusion until it reaches the location $x^\star$ where its velocity equals the ambient spatially dependent velocity of the chaotic stirring $-x^\star$.

It has been observed for both models in [14] that there is a critical Damköhler number such that no stationary pulses exist for $Da < Da_c$, i.e. when the time scale of the chaotic advection, $\tau_f = 1/\lambda$, becomes too fast with respect to the time scale of the reaction, $t_r = 1/k$. For large Damköhler numbers, an asymptotic expression for the scaling of the total concentration was developed in [14]. However, these techniques cannot describe the behaviour close to the bifurcation point. It is this saddle node bifurcation we are mainly concerned with in this work.

3 Nonperturbative method

A method was developed in [20] to study critical wave propagation of single pulses and pulse trains in excitable media in one and two dimensions. It was based on the observation that close to the bifurcation point the pulse shape is approximately a bell-shaped function. Numerical simulations show that this is the case for both systems, (3) and (4), close to the bifurcation point at Da_c. A test function approximation that optimises the two free parameters of a bell-shaped function, i.e. its amplitude and its width, allows us to find the actual bifurcation point, Da_c, and determine the pulse shape for close-to-critical pulses at Damköhler numbers near Da_c. We note that the framework of asymptotic techniques, such as inner and outer expansions where the solution is separated into a steep narrow front and a flat plateau, are bound to fail close to the bifurcation point as the pulse is clearly bell-shaped, and such a separation is not possible anymore. We shall make explicit use of the shape of the pulse close to the critical point and parameterise the pulse appropriately, as is done in the method of collective coordinates in the studies of solitary waves [26].

We choose c of the general form

$$c(x) = f_0 C(\eta) \qquad \text{with} \qquad \eta = wx \,, \tag{5}$$

where $C(\eta)$ is a symmetric, bell-shaped function (a Gaussian, for example) of unit width and height, and f_0 is the amplitude of the pulse. Numerical simulations reveal that close to the saddle node, the solution is asymptotically given by a Gaussian. However, our result does not depend on the specific choice of the test function, and the numerical values differ only marginally when *sech*-functions are used. We restrict the solutions to a subspace of a bell-shaped function $C(\eta)$, which is parameterised by the amplitude, f_0, and the inverse pulse width, w. These parameters are determined by minimizing the error made by the restriction to the subspace defined by (5). This is achieved by projecting Eq. (3) (or (4)), onto the tangent space of the restricted subspace, which is spanned by $\partial c/\partial f_0 = C$ and $\partial c/\partial w = \eta C_\eta / w$. This assures that the error made by restricting the solution space to the test functions is minimized. We set the integral of the product of Eq. (3) (or (4)) with the basis functions of the tangent space (over the entire η-domain) to zero. This will lead to algebraic equations for the amplitude, f_0, and the inverse pulse width, w, and also yield the critical Damköhler number Da_c.

Moreover, for the solution behaviour at large Damköhler numbers far way from the bifurcation point, where the solution takes the shape of a well defined front, we may use a superposition of tanh-functions for the test function $C(\eta)$. Here the free parameters are the inverse width of the interface and the total width of the front. We can apply the same technique to determine these two free parameters. This will be attempted in Section 5.

4 Behaviour close to the saddle node bifurcation

In this Section we apply the technique described in the previous Section to describe the behaviour near the saddle node bifurcation where the solution is well approximated by a bell-shaped function with two free parameters, namely the amplitude f_0 and the inverse pulse width w. This is a purely numerical observation and has no further analytical justification.

4.1 Autocatalytic system

We first investigate the autocatalytic system (3). As has been first observed numerically in [14], steady solutions to the one-dimensional problem can be obtained for values of $Da > Da_c$. As we approach the bifurcation point the amplitudes of the solutions to the autocatalytic reaction decrease to zero (see Fig. 1). Conversely, with increasing Damköhler number the pulse width increases and the maximal amplitude saturates around $c(x) = 1$. Here, the solution is a regular front solution with a well defined plateau and a narrow steep front.

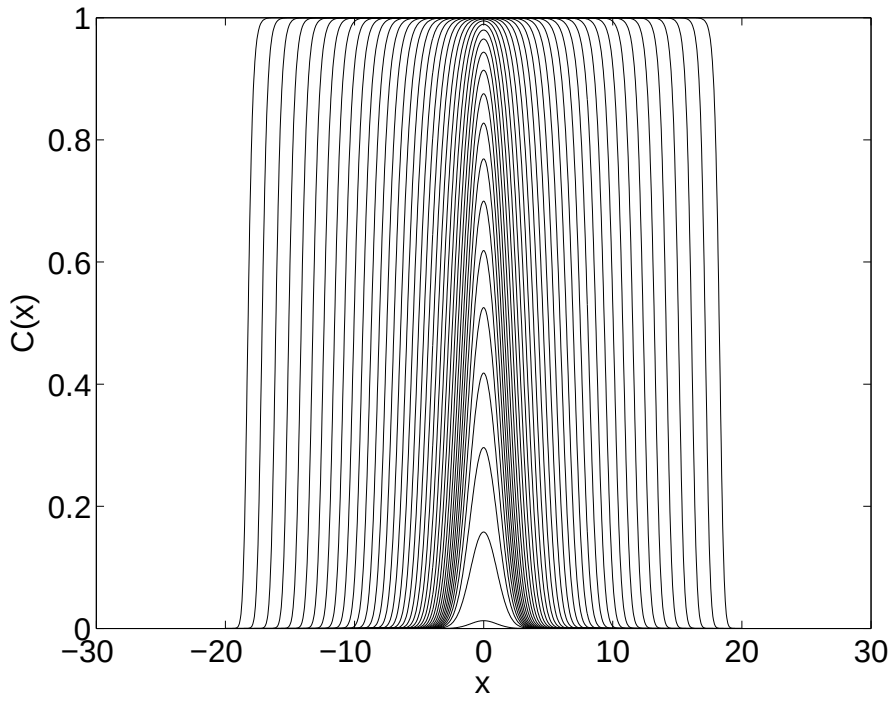

Figure 1: The steady solutions of the autocatalytic reaction for logarithmically spaced values of Da between $Da = Da_c(= 1)$ and Da=100.

We are interested in steady-state solutions and set $\partial c/\partial t = 0$ in (3). We obtain the ordinary differential equation

$$w^2 \frac{\partial^2 C}{\partial \eta^2} + \eta \frac{\partial C}{\partial \eta} + Da\, C(1 - f_0 C) = 0\,, \tag{6}$$

where $\eta = wx$. As described in Section 3 we need to project equation (6) onto the tangent space of the restricted solution submanifold. We require

$$\langle w^2 C_{\eta\eta} + \eta C_\eta + Da\, C(1 - f_0 C) \mid C \rangle = 0, \tag{7}$$

$$\langle w^2 C_{\eta\eta} + \eta C_\eta + Da\, C(1 - f_0 C) \mid \eta C_\eta \rangle = 0, \tag{8}$$

where the brackets indicate integration over the whole η-domain. Using $\langle C_{\eta\eta} C \rangle = -\langle C_\eta^2 \rangle = 2\langle \eta C_{\eta\eta} C_\eta \rangle$, and $\langle \eta C_\eta C^a \rangle = -\langle C^{a+1} \rangle / (a+1)$, we can simplify the set of equations to get an expression for the amplitude of the form

$$f_0 = \frac{1}{\langle C^3 \rangle} \frac{3}{5Da} \left(\langle C^2 \rangle \left(\frac{4Da - 1}{2} \right) - 2\langle \eta^2 C_\eta^2 \rangle \right).$$

Choosing a Gaussian test function $C = \exp(-\eta^2)$, this reduces further to

$$f_0 = \frac{3\sqrt{6}}{5} \left(\frac{Da - 1}{Da} \right)\,. \tag{9}$$

This immediately yields the critical Damköhler number $Da_c = 1$ which is verified by numerical simulation of the full autocatalytic system (3) (see Fig. 2b).

Using the result (9) for the amplitude f_0 we can calculate the inverse pulse width w from either (7) or (8). We obtain

$$w = \sqrt{\frac{7 - 2Da}{10}}. \tag{10}$$

For values of $Da > 3.5$ equation (10) yields purely imaginary values indicating that our method breaks down, and that at these Damköhler numbers the solution cannot be approximated by a bell-shaped function anymore. We note that the value of the Damköhler number where the solution has 'saturated' to become a front-like solution (see Fig. 1) is at $Da \approx 10$. However, the solution looses its bell-shaped character before that 'saturation' point.

Fig. 2 shows a comparison of our analytical results (9,10) with numerical simulations of (3). The analytical results for the amplitude fit progressively better as we approach the saddle node, corresponding to the fact that the solution is well approximated by a bell-shaped function the closer it is to the saddle node.

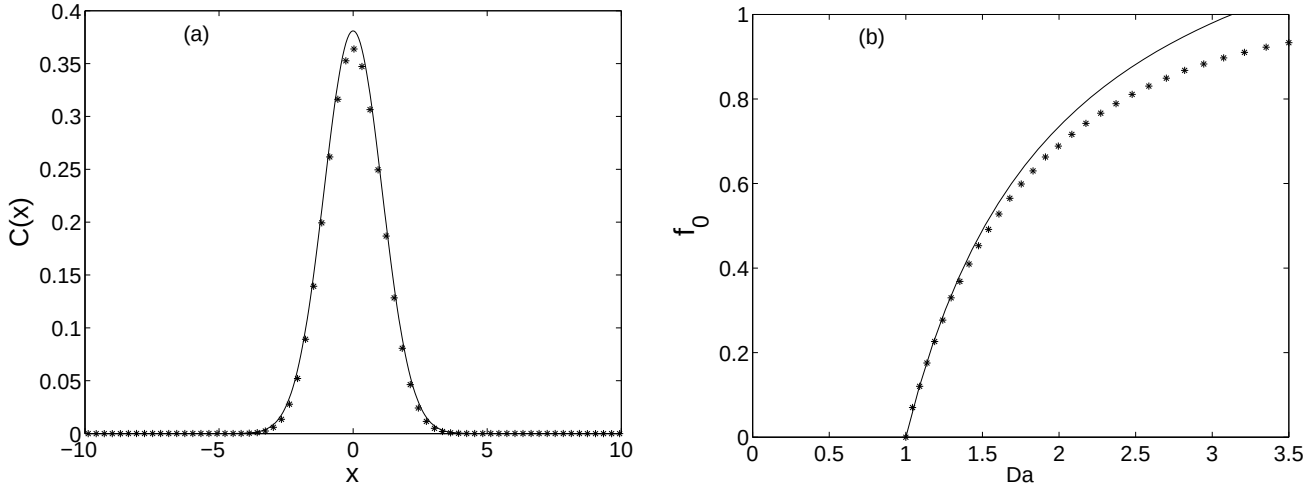

Figure 2: Comparison of numerical simulations of our analytical results (continuous lines) with the autocatalytic model equation (3). (a): Pulse $c(x)$ at $Da = 1.35$. (b): Pulse amplitude f_0 versus Damköhler number Da. The continuous line is our analytical result for the stable branch of the saddle node bifurcation (9).

4.2 Bistable system

We can apply the same methodology used in Sec. 4.1 to the bistable system (4). The steady solutions of the bistable system have the same behaviour as those in the autocatalytic system (3). Close to the bifurcation point at Da_c the solution takes the form of a bell-shaped function (see Fig. 3). Whereas the solution approaches a front solution for higher values of the Damköhler number as is evidenced in Fig. 3.

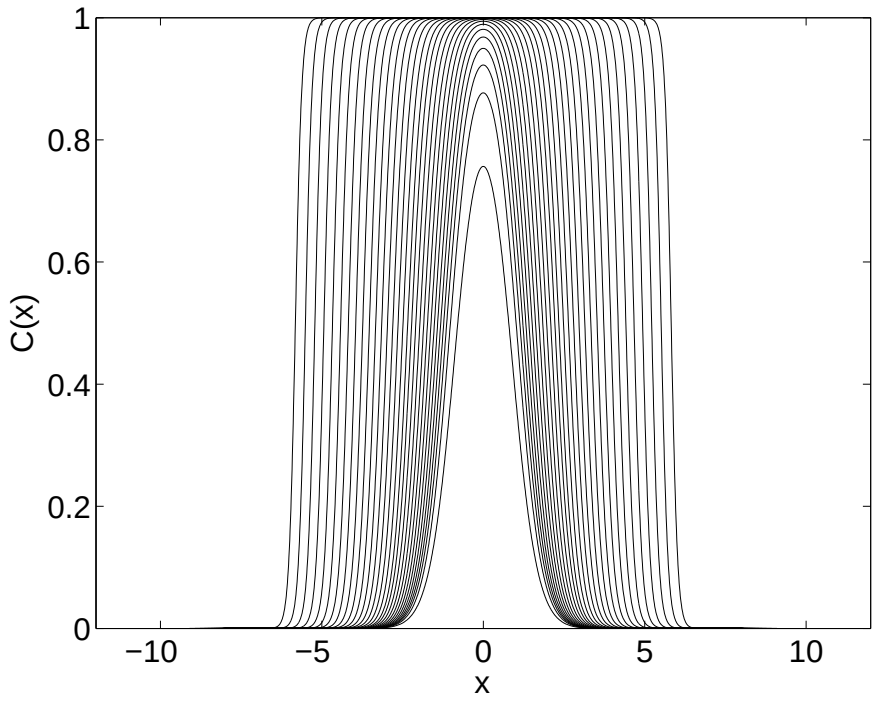

Figure 3: The steady solutions of the bistable reaction with $\alpha = 0.2$ for logarithmically spaced values of Da between $Da = Da_c$ and $Da = 1000$.

As in Sec. 4.1, we look at stationary front solutions and study of (4), and consider

$$w^2 \frac{d^2C}{d\eta^2} + \eta \frac{dC}{d\eta} + Da\, C(\alpha - f_0 C)(f_0 C - 1) = 0\,. \tag{11}$$

Integrating the product of (11) with C and with $\eta \partial C/\partial \eta$ over the η-domain leads to expressions for the amplitude f_0 and the inverse width w.

We obtain a quadratic equation for the amplitude,

$$A f_0^2 + B f_0 + C = 0, \tag{12}$$

where, as before, the coefficients can be obtained explicitly for a specific choice of test function. Choosing a Gaussian test function, we have

$$A = \frac{3}{4}\,, \quad B = \frac{-5\,(1+\alpha)}{3\sqrt{3}}\,, \quad C = \frac{\sqrt{2}\,(1 + Da\;\alpha)}{Da}\,. \tag{13}$$

This yields two solutions for the amplitude f_0, one corresponding to a stable branch and one corresponding to an unstable branch. These two branches collide at the critical Damköhler number and disappear via a saddle node bifurcation. An expression for the critical Damköhler number for any given value of α can be obtained from (12), with the condition $B^2 - 4AC = 0$. We find that

$$Da_c = \frac{1}{q(1+\alpha)^2 - \alpha} \quad \text{with} \quad q = \frac{25}{81\sqrt{2}}\,.$$

This poses an upper bound for α

$$\alpha_{max} = \frac{1 - 2q - \sqrt{1 - 4q}}{2q},$$

which is approximately $\alpha_{max} \approx 0.4744$. Hence the chaotic stirring changes the Maxwell point which in the non-stirred case is at $\alpha = 0.5$.
As in Section 4.1 the inverse width can be calculated as well.

In Fig. 4 we show a comparison of our analytical results (12,13) with numerical simulations of (11). In Fig. 4 we see that the correspondence of our analytical results with the numerical simulation of the full system (11) is much better for the unstable branch than for the stable branch. As a matter of fact, the unstable solutions obtained by integrating (11) by means of a shooting method stay close to a bell-shaped function even far away from the bifurcation point at $Da = Da_c$.

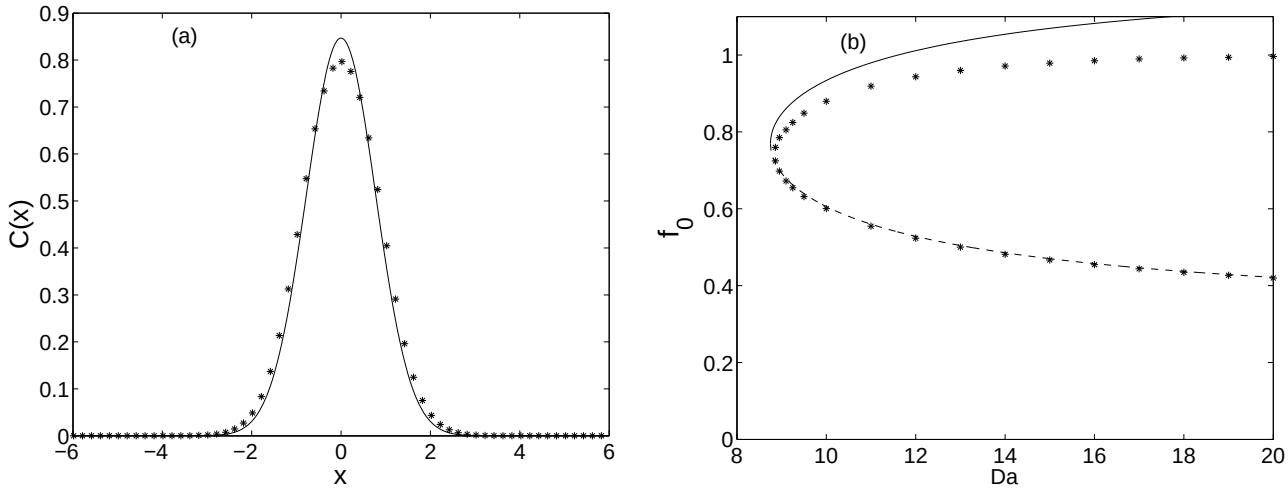

Figure 4: Comparison of numerical simulations of our analytical results (continuous lines) with the bistable model equation (11) solved by a shooting method. (a): Pulse $c(x)$ at $Da = 9$. (b): Pulse amplitude f_0 versus Damköhler number Da. The continuous line and the dashed line show the stable and the unstable branch, respectively, of the saddle node bifurcation according to our analytical result (12).

5 Behaviour far away from the bifurcation

In this Section we apply the technique described in Section 3 to describe the behaviour far away from the saddle node bifurcation. For large Damköhler numbers the solution is not bell-shaped anymore but instead becomes a front solution with a well defined plateau (see Fig. 1 and Fig. 3). Numerical simulations show that the solution in this regime is well approximated by a test function of the following form

$$C(x) = \frac{1}{2}\left(\tanh\left(w(x+\nu)\right) - \tanh\left(w(x-\nu)\right)\right) \ . \tag{14}$$

Again we have two free parameters, namely the total width ν and the inverse interface width w. This, in principle, provides two conditions by projecting onto the tangent space of the restricted solution space spanned by $\partial C/\partial w$ and $\partial C/\partial \nu$. These two conditions allow us to determine w and ν.

In the literature of lamellar one-dimensional model equations one encounters the following phenomenological argument for the location of the front. We recall that a stationary front is given through a balance of the front velocity v with the velocity of the chaotic stirring x. The front has a zero velocity when $v = x$, which implies $v = \nu$. If we now approximate the front velocity v by its unstirred value, we can calculate v as a function of the Damköhler number.

Our non-perturbative technique is able to deduce this phenomenological formula for the front width ν for both cases, the autocatalytic and the bistable case. The agreement between our theory and the phenomenological formulae is accurate up to 0.1%. For simplicity we therefore use in the following Sections the phenomenological argument to close the equations.

5.1 Autocatalytic system

For the autocatalytic system (3), the front velocity for the unstirred case is given by $v = 2\sqrt{Da}$ (provided that the initial condition is of a form such as (14) [23, 24]). Hence the phenomenological argument yields

$$\nu = 2\sqrt{Da}\ . \tag{15}$$

Fig. 5(a) shows that the phenomenological argument indeed is a good approximation. We note again, that our non-perturbative theory shows very good agreement with the phenomenological formula (15).

Equation (15) can now be used to close one of the two conditions of the projection method. Without loss of generality, we choose the projection onto $\partial C/\partial w$. The resulting equation is

$$\langle w^2 C_{\eta\eta} + \eta C_\eta + Da\, C(1-C) \mid \eta C_\eta \rangle = 0\ . \tag{16}$$

Here we choose (14) as a test function and express ν by (15). The resulting equation for w is transcendental and we need to evaluate it numerically.

In Fig. 5(b) a comparison of our result with the numerical simulation of (3) is shown.

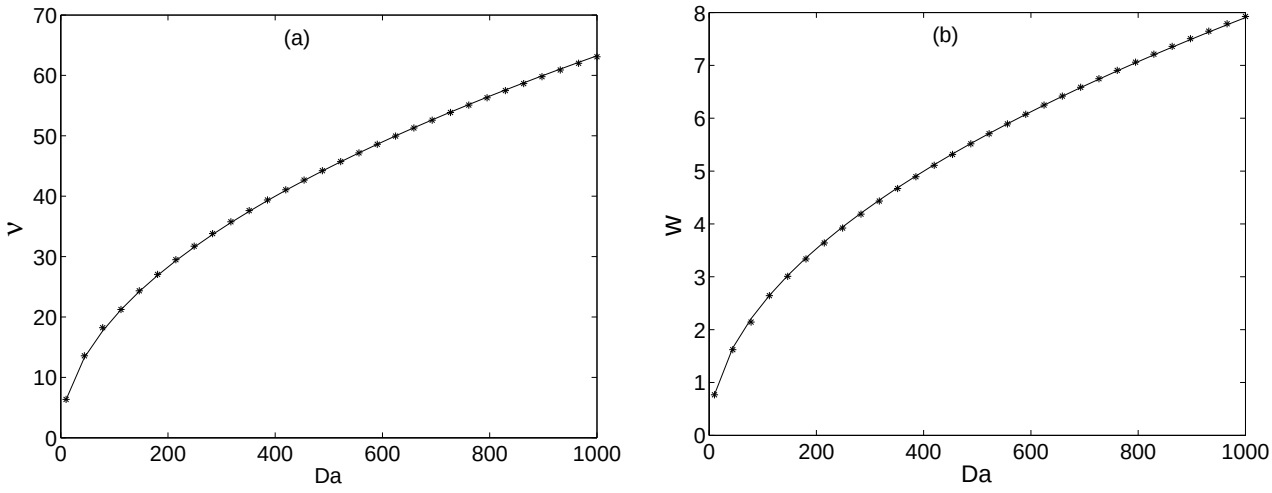

Figure 5: Solution behaviour for large Damköhler numbers Da far away from the saddle node bifurcation. Numerical simulations of the full autocatalytic system (3) are depicted by stars; the analytical results are depicted by continuous lines. (a): Total width ν as a function of the Damköhler number. The continuous line shows the phenomenological formula (15). (b): Inverse interface width w as a function of the Damköhler number. The continuous line shows our analytical result.

5.2 Bistable system

For the bistable system, the front velocity for the unstirred case is given by $v = \sqrt{2Da}\left(\frac{1}{2} - \alpha\right)$ [23, 24]. Hence our phenomenological argument now yields

$$\nu = \sqrt{2Da}\left(\frac{1}{2} - \alpha\right) \ . \tag{17}$$

Fig. 6(a) shows again good agreement of the phenomenological argument with the actual dynamics of the full system.

Again, equation (17) can be used to calculate the inverse interface width w from the condition that the projection of equation (4) onto $\partial C/\partial w$ vanishes. This condition is given by

$$\langle w^2 C_{\eta\eta} + \eta C_\eta + Da\, C(\alpha - C)(C - 1) \mid \eta C_\eta \rangle = 0, \tag{18}$$

where, as above, we use (14) as a test function, and express ν by (17). As for the autocatalytic system, the inverse width w can only be given by numerically evaluating (18).

In Fig. 6(b) a comparison of our result with the numerical simulation of (4) is shown.

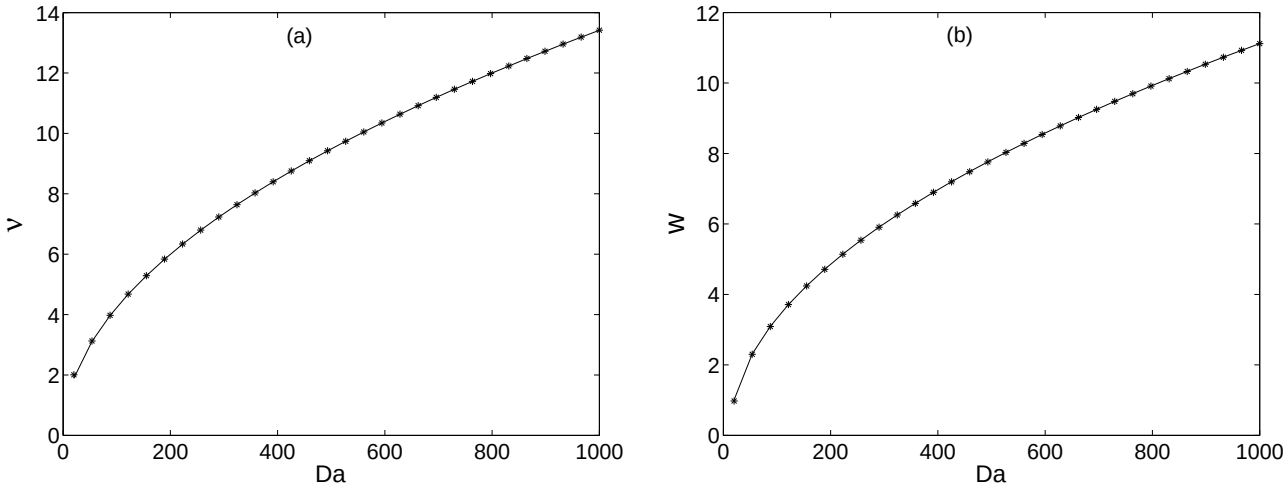

Figure 6: Solution behaviour for large Damköhler numbers Da far away from the saddle node bifurcation. Numerical simulations of the full bistable system (4) are depicted by stars; the analytical results are depicted by continuous lines. (a): Total width ν as a function of the Damköhler number. The continuous line shows the phenomenological formula (17). (b): Inverse interface width w as a function of the Damköhler number. The continuous line shows our analytical result (18).

6 Summary and discussion

We studied the solution behaviour near the saddle node bifurcation which occur in one-dimensional simplified models of reaction-diffusion equations subjected to chaotic advection. The interplay of reaction dynamics with the chaotic stirring leads to stationary fronts in the one-dimensional model equation corresponding to filaments with a well-defined width in the full two-dimensional system. Depending on the Damköhler number which measures the ratio of the time scales of the chaotic fluid motion and the reaction kinetics, the system undergoes a saddle bifurcation when the fluid motion is much faster than the reaction kinetics.

We applied a technique originally developed for excitable media [20] to study this saddle node bifurcation. We determined the critical Damköhler number and described the solution close to the bifurcation point with good agreement with numerical simulations of the full partial differential equations.

By choosing a front-shaped test function we were able to apply the technique originally developed to study behaviour close to the saddle node bifurcation to describe fully developed fronts far away from the bifurcation point. The two conditions given by the variational technique for the two free parameters of such a stationary front, i.e. its inverse interface width w and its total width ν, reproduced accurately the numerical results. Moreover, we were able to reproduce a widely used phenomenological argument, relating the front-width to the front velocity of the unstirred case. A comparison with numerical

simulations justified our approach.

Acknowledgements G.A.G gratefully acknowledges support by the Australian Research Council, DP0452147. S.N.M was supported by a University of Sydney Postgraduate award. We would like to thank Stephen Cox for valuable discussions.

References

[1] I. R. Epstein, Nature **374**, 321 (1995).

[2] M. A. Allen, J. Brindley, J. Merkin and M. J. Piling, Phys. Rev. E **54**, 2140 (1996).

[3] E. R. Abraham, Nature **391**, 577 (1998).

[4] A. P. Martin, J. Plank. Res. **22**, 597 (2000).

[5] P. McLeod, A. P. Martin and K. J. Richards, Ecological Modelling **158**, 111 (2002).

[6] E. Hernández-García and C. Lopéz, Sustained plankton blooms under open chaotic flows, Ecological Complexity **1**, 193 (2004).

[7] S. Edouard, B. Legras, F. Lefévre and R. Eymard, Nature **384**, 444 (1996).

[8] A. Rovinsky and M. Menzinger, Phys. Rev. Lett. **69**, 1193 (1992).

[9] C. Zhou, J. Kurths, Z. Neufeld and I. Z. Kiss, Phys. Rev. Lett. **91**, 150601 (2003).

[10] Z. Neufeld, I. Z. Kiss, C. Zhou and J. Kurths, Phys. Rev. Lett. **91**, 084101 (2003).

[11] W. R. Young, A. J. Roberts and G. Stuhne, Nature **412**, 328 (2001).

[12] G. Metcalfe and J. M. Ottino, Phys. Rev. Lett. **72**, 2875 (1994).

[13] Z. Neufeld, Phys. Rev. Lett. **87**, 108301 (2001).

[14] Z. Neufeld, P. H. Haynes and T. Tél, Chaos **12**, 426 (2002).

[15] Z. Neufeld, C. Lopéz, E. Hernández-García and O. Piro, Phys. Rev. E **66**, 066208 (2002).

[16] E. Hernández-García, C. Lopéz and Z. Neufeld, Physica A **327**, 59 (2003).

[17] I. Z. Kiss, J. H. Merkin and Z. Neufeld, Physica D **183**, 175 (2003).

[18] I. Z. Kiss, J. H. Merkin, S. K. Scott, P. L. Simon, S.Kalliadasis and Z. Neufeld, Physica D **176**, 67 (2003).

[19] X. Z. Tang and A. H. Boozer, Chaos **9**, 183 (1999).

[20] G. A. Gottwald and L. Kramer, Chaos **14**, 855 (2004).

[21] R. A. Fisher, Ann. Eugenics **7**, 353 (1937).

[22] A. Kolomogorov, I. Petrovsky and N. Piscounoff, Moscow Univ. Math. Bull. **1**, 1 (1937).

[23] J. D. Murray, *Mathematical Biology*, 2nd edition (Springer Verlag, New York, 1993).

[24] J. Keener and J. Sneyd, *Mathematical Physiology* (Springer Verlag, New York, 1998).

[25] A. S. Mikhailov, *Foundations of synergetics I: Distributed active systems*, 2nd edition (Springer Verlag, Berlin, 1994).

[26] A. Scott, *Nonlinear Science - Emergence and Dynamics of Coherent Structures* (Oxford University Press, Oxford, 1999).